Jordan Journal of Civil Engineering, Volume **20**, No. **3**, **2026**
DOI: https://doi.org/10.14525/JJCE.v20i3.09

Jordan Journal of Civil Engineering

Journal homepage: https://jjce.just.edu.jo

Influence of Pile Geometry and Soil–Pile Interface on the Uplift Performance of Tension Piles Embedded in Dry Sand

Deman Rahman Majeed [1)], ***Zahraa Noori Rashied*** [1)]

[1)] *Department of Geotechnical Engineering, Faculty of Engineering, Koya University, Koya 44023, Kurdistan Region – F.R. Iraq.*

ARTICLE INFO

Article History:
Received: 5/10/2025
Accepted: 12/2/2026

ABSTRACT

This study aims to investigate how soil relative density, pile slenderness ratio (L/D), and soil–pile interface roughness jointly influence the uplift performance of straight-shaft tension piles embedded in dry sand. A comprehensive series of 27 laboratory pullout tests was performed to measure how these factors interact in determining uplift capacity and displacement behavior. The findings indicate that an increase in L/D yields the most substantial enhancement in uplift resistance, with the highest gains observed at L/D = 30. The roughness of the interface contributes moderately to capacity enhancement, while the influence of soil density, although secondary, remains significant, especially in dense sand paired with rough and medium-rough interfaces. The ratio of interface friction to internal friction (δ/ϕ) rises with increased surface roughness; however, dense sand with rough surfaces demonstrates slight reductions due to strain softening. The ultimate uplift capacity was observed to mobilize at displacements between 2.6% and 44.5% of the pile diameter, emphasizing the importance of considering allowable displacement limits in design. The combination of soil density, pile roughness, and slenderness ratio significantly influences the failure mode (brittle or ductile). This study highlights the combined and relative effects of geometry, soil density, and interface conditions, offering new perspectives for more dependable tension pile design in sandy soils.

Keywords: Uplift capacity, Vertical displacement, Straight shaft piles, Pile geometry, Interface roughness, Relative density.

INTRODUCTION

Tension piles are widely used to resist uplift forces generated by buoyancy, overturning moments, wind, and seismic loading in civil and geotechnical structures. Tension piles, also termed uplift or anchor piles, are commonly installed in offshore platforms, transmission towers, buried pipelines, and retaining systems to counteract upward or overturning loads (Das, 2019). Unlike compressive piles, tension piles mobilize resistance primarily through shaft friction rather than end bearing. The behavior of pile shaft resistance under tension loading is complex and not yet fully understood. Extensive studies have been conducted, but many have focused on a limited number of parameters (Meyerhof & Adams, 1968; Ismael, 1989; Alawneh et al., 1999; Al-Mhidib & Edil, 1999; Srivastava et al., 2008; Azzam & Al Mesmary, 2010; Gaaver, 2013; Kranthikumar et al., 2016; Azzam & Elwakil, 2016; Azzam & Basha, 2017). Limited studies focus on observing the effects of numerous parameters on the performance of tension piles (Shanker et al., 2007; Azzam & Basha, 2018; You et al., 2024). Understanding the combined effect of more than two parameters, like pile geometry, soil density and

pile-soil interface interaction, is essential for reliable performance prediction and cost-effective engineering solutions.

Das and Rozendal (1983) examined the uplift capacity of piles installed in dry sand and demonstrated that unit skin friction increases with depth up to a certain distance, then remains constant. Also, they concluded that both pile embedment depth and soil compaction play crucial roles in determining uplift capacity. Additionally, a study by Alawneh (1999) formulated a method for estimating the ultimate uplift shaft resistance of driven piles in sandy soil, taking into account the reduction of shaft friction that occurs during installation. This method also correlates the maximum earth pressure coefficient with variables, including the relative density of the sand and the diameter of the pile. Alawneh et al. (1999) demonstrated through experimental methods that the primary factors influencing the measured unit shaft resistance during ultimate uplift are the pile placement technique and the relative density of the sand. Other factors, including the type of pile end and the roughness of the pile surface, have less effects. Some of the authors reported that the installation method of piles in the soil and the type of load affect the shaft resistance of a single pile (Franke & Muth, 1985; Ismael, 1989; Ghaly et al., 1992). Marumdee (2013) conducted a comparison of three methods (Kulhawy et al. (1979), Das (1983), and Chattopadhyay and Pise (1986)) to estimate the ultimate uplift capacity of piles in sandy soil. The findings indicated that the methods yielded different results, highlighting the importance of meticulously choosing estimation techniques according to the particular conditions of each project. Shanker et al. (2007) created a simple semi-empirical model to assess the uplift capacity of piles installed in dry sand. This model takes into account various parameters related to both the piles and the soil, integrating theoretical and practical elements that demonstrate a strong correlation with data obtained from existing literature and model testing. An enhancement in the relative density of soil, along with an increase in the ratio of pile embedment depth to diameter (L/d), significantly boosts the net uplift capacity of an individual pile (Gaaver, 2013; Parthipan, 2017). Basha and Azzam (2018) studied the effect of various parameters, including soil relative density, submerged pile depth, and pile slenderness ratio, on tension pile capacity experimentally and depicted that when the submerged pile length ratio is increased, the uplift capacity of a single pile decreases. Furthermore, van Baars and Niekerk (2019) showed numerically that the way in which the soil and pile behave virtually has a big impact on how the pile behaves. The uplift load bearing capacity rises exponentially with an increase in base diameter to pile shaft diameter and progressively or linearly with an increase in pile length to pile shaft ratio. Alawneh et al. (2019) utilized well-documented field cases to validate their introduced novel design methodology for assessing the tensile strength of dynamically driven closed-ended piles in cohesionless soils, which was subsequently adapted for open-ended piles using three distinct methods (plug indicator, transforming the open-ended pile into an equivalent solid pile and combined method). They demonstrated that the plug indicator method provided the closest correlation with the measured capacities. In contrast to loose sand, dense sand has a higher pile pullout capacity; nonetheless, vertical displacements in dense sand are catastrophic, whereas they are gradual in loose sand (Devashish Babulal Kumavat, 2020). You et al. (2024) examined how the soil fines content and the shear resistance properties of the pile-soil interface affect the pullout resistance. They emphasized the importance of assessing the roles of interface friction angle, cohesion (or adhesion) at the shear surface and fines content of the soil on predicting of pile pullout resistance.

This work aims to investigate the combined effect of soil relative density (dense, medium and loose), pile slenderness (L/D) ratio (10, 20 and 30) and interface friction (smooth, medium, rough pile surface) on the uplift capacity of a straight shaft pile. The combined effects of these parameters on tension pile performance during uplift events are not fully understood yet.

MATERIALS AND EXPERIMENTAL METHODOLOGY

Soil Preparation and Physical Characteristics

In this research, the used soil in the experimental program was clean dust free sand collected from Ranya, Sulaymaniyah, Iraq. The soil initially passes through sieve No. 16, which has a maximum size of 1.18 mm. To determine the physical characteristics of soil, including its specific gravity, grain size analysis, and maximum and minimum dry densities, tests were conducted according to American Society of Testing Materials (ASTM). Table 1 summarizes the physical

characteristics of soil, while the grain size distribution (ASTM D422–63*)* is shown in Figure 1. The soil is classified as poorly graded sand according to the Unified Soil Classification System (USCS).

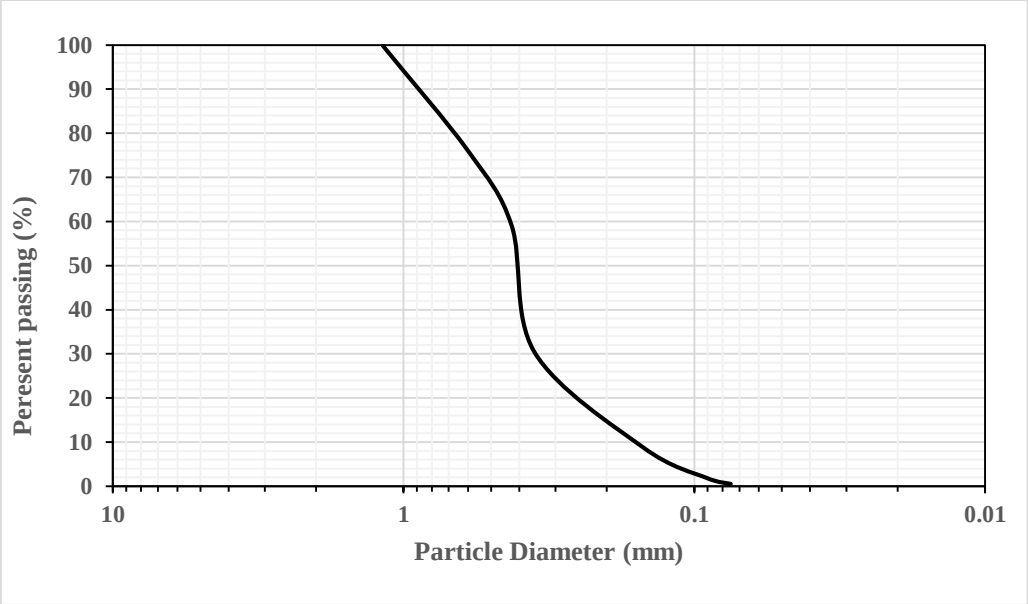

Figure 1. Grain size analysis

Table 1. Physical properties of the soil

Soil Property	Value	Standard of Test
Specific Gravity, (G_S)	2.65	ASTM D854 (2014)
Max. Unit Weight, γ_{max} (kN/m^3)	17.6	ASTM D 4253 (2000)
Min. Unit Weight, γ_{min} (kN/m^3)	15.21	ASTM D 4254 (2000)
Max. Void Ratio, e_{max}	0.709	
Min. Void Ratio, e_{min}	0.477	
Effective grain size, D_{10} (mm)	0.17	
Average grain size, D_{30} (mm)	0.36	
Average grain size, D_{60} (mm)	0.44	
Coefficient of Uniformity, Cu	2.589	
Coefficient of Curvature, Cc	1.73	
Soil Classification (USCS)	Poorly- graded sand, (SP)	ASTM D2487 (2010)

Pile Models and Pullout Device

Nine circular steel model piles were prepared to meet the objectives of this study at three different L/D ratios (10, 20, and 30) and three different interface roughness degrees (smooth, medium and rough), as shown in Figure 2. All of the modeled piles have an average diameter (D) of 15 mm. According to their length, the piles can be categorized into three groups, the first one has 150 mm, the second 300 mm and the third 450 mm length. The ratio between the pile diameter (D) to the average grain size (D_{50}) has to be greater than 30 to discard the scale effect (Franke & Muth, 1985). The ratio (D/D_{50}) of 37.5 was achieved in this study as the average grain size of the used soil D_{50} = 0.40 mm (see Figure 1). Regarding the interface roughness, smooth steel piles were used to simulate a smooth interface (S), while sandpaper grit 220 and grit 100 were used to coat the model piles to demonstrate the medium (U) and rough (R) soil-pile interface, respectively. The three roughness categories were selected to simulate real field conditions. Smooth interface simulates driven steel piles or coated piles where surface friction is lower, while medium interface (grit 220) simulates concrete piles or lightly roughened steel, and rough interface simulates

bored piles, roughened cast-in-place piles, or piles in sand with higher dilation resistance (Lepage & Boulon, 2010; Tehrani et al., 2016). To facilitate the measurement of the pullout load and upward displacement, a steel plate measuring (50×50×3) mm with an eyehook was well welded to the pile head.

The pullout device consists of a testing tank and a loading frame, as shown in Figure 3. A smooth, rigid plastic testing tank (4 mm thickness) with an average inside cross-sectional area of (400 × 400) mm and 600 mm in height was used. The testing tank dimensions were selected to avoid boundary effects (Nazir, 2008; Shark & Patra, 2008; Basha & Azzam, 2018). To conduct a pullout test for each individual model pile, a steel loading frame of 1250 mm height and 800 mm width supported by a (1100 × 1100) mm base resting on (200 × 200) mm four square steel pads to raise it above the ground about 150 mm was manufactured. An extension bar of 400 mm length was located at a height of 650 mm from the ground to support the dial gauge (0.01 mm per division precision), to record the vertical displacement of the pile due to the applied uplift load. A weight holder was placed in order to apply an uplift load connected to a steel wire (2 mm diameter) going through two freely rotated pulleys, one of them placed at the center of the frame and the other one placed at the end of a 300 mm horizontal side extension. The second end of the steel wire was connected to the eyehook on the pile top.

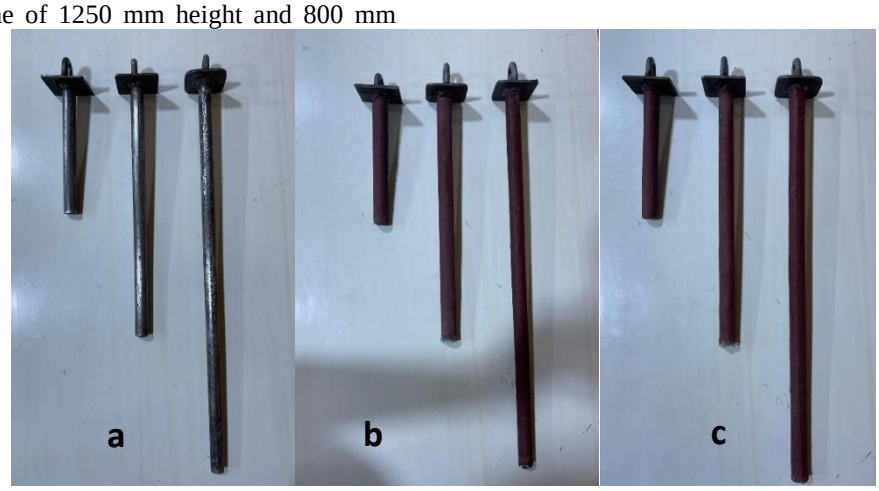

Figure 2. Various geometry ratio (L/D) and skin roughness modeled Piles: a) Smooth skin; b) Medium skin and c) Rough skin

Figure 3. Pullout device and testing tank

Test Program and Procedure

The testing program in this research was carried out by conducting a series of laboratory pullout tests under pure axial pullout loads to study the behavior of tension piles embedded in dry poorly graded sand due to different geometry parameters (L/D), sand relative density (D_r) and soil-pile interface. The parameters were varied to evaluate their effects on the uplift capacity of single piles. The selected parameters were categorized into three groups. The first group consists of three relative densities (15%, 60% and 90%) used to simulate loose, medium and dense sand states. The second one includes three pile-soil interfaces as a function of pile skin roughness. Furthermore, the three pile slenderness (L/D) values were categorized as a third group. Table 2 shows a summary of the testing program with the identification test code for each case. The letters L, M and D are used to define the states of soil (loose, medium and dense), respectively. The letters S, U and R are used to define the pile skin roughness (smooth, medium and rough). To prevent repetition in the identification symbols of medium density and medium roughness, the letter U was used to define medium skin roughness.

To obtain a loose soil state, dry sand was poured gently into a testing tank using a funnel to ensure uniform distribution, while the medium and dense states were achieved through tamping. In order to gain the desired density, the sand was uniformly distributed and manually tamped in layers of 50 mm thickness to a weight accuracy of 0.01 kg (Al-Mhidib & Edil, 1999). After preparing the soil for each individual state, the model pile was driven into the sand carefully to reduce the soil disturbance (Robinsky, 1964) and left for over 48 hrs to gain relaxation between the pile skin and the soil grains before conducting the pullout test. Then, the uplift load is applied by incremental adding of dead weights. The dial gauge reading and the corresponding load increments were recorded if the difference between two dial gage readings was not more than 0.01 mm per 5 minutes.

Table 2. Testing program

Soil State	Pile Interface Roughness	Geometry Parameters (L/D)	Test Code	No. of Tests
Loose (L)	**Smooth (S)**	10, 20, 30	LS10, LS20, LS30	27
	Medium (U)	10, 20, 30	LU10, LU20, LU30	
	Rough (R)	10, 20, 30	LR10, LR20, LR30	
Medium (M)	**Smooth (S)**	10, 20, 30	MS10, MS20, MS30	
	Medium (U)	10, 20, 30	MU10, MU20, MU30	
	Rough (R)	10, 20, 30	MR10, MR20, MR30	
Dense (D)	**Smooth (S)**	10, 20, 30	DS10, DS20, DS30	
	Medium (U)	10, 20, 30	DU10, DU20, DU30	
	Rough (R)	10, 20, 30	DR10, DR20, DR30	

RESULTS AND DISCUSSION

Pile-Soil Interface Friction

In this sub-section, the combined effect of three different relative densities (15, 60 and 90%) and three pile skin roughness degrees (smooth, medium and rough) on the interface friction angle was observed. The direct shear test according to ASTM D3080M (2011) was carried out using 0.5 mm/min strain rate to evaluate the angle of internal friction (ϕ) and the interface friction angle (δ) for all soil-soil and pile-soil states. Three (6 × 6 × 1.5) cm steel pads were used to model the soil-pile interface (see Figure 4), one of them coated with grit 220 sand paper (medium roughness) and another covered with grit 100 sand paper (rough skin), then a direct shear test was conducted by sliding the soil over the steel pad. Summary of the internal angle of friction and the interface friction angle at different densities and interface roughness degrees given in Table 3. The results demonstrate that there is a noticeable increase in the interface friction angle in accordance with the increase in soil density and interface roughness. However, the (δ/ϕ) ratio exhibits an increase in accordance to increasing pile skin roughness, with no significant effect on the change in relative density for a proper roughness state, except for the reduction observed in the state

representing dense soil–rough skin (see Figure 5). A reduction of (δ/ϕ) in dense soils with rough pile surfaces indicates strain-softening behavior. The pile initially mobilizes high interface friction, but as displacement increases, the mobilized friction gradually decreases. This is particularly observed in dense sands, where particle rearrangement and local dilation reduce the effective interface resistance after peak mobilization (White & Lehane, 2004; Lehane & White, 2005; Chen et al., 2022).

Table 3. Internal friction angle (ϕ°) and interface friction angle (δ°)

Interface State	Friction Angle	Pile Skin Roughness	Soil State		
			Loose (L)	Medium (M)	Dense(D)
Soil-Soil	**(ϕ°)**	-	32.90	37.20	40.26
Soil-Pile	**(δ°)**	Smooth (S)	28.40	33.10	35.50
		Medium (M)	33.49	37.80	41.42
		Rough (R)	35.29	40.50	41.60

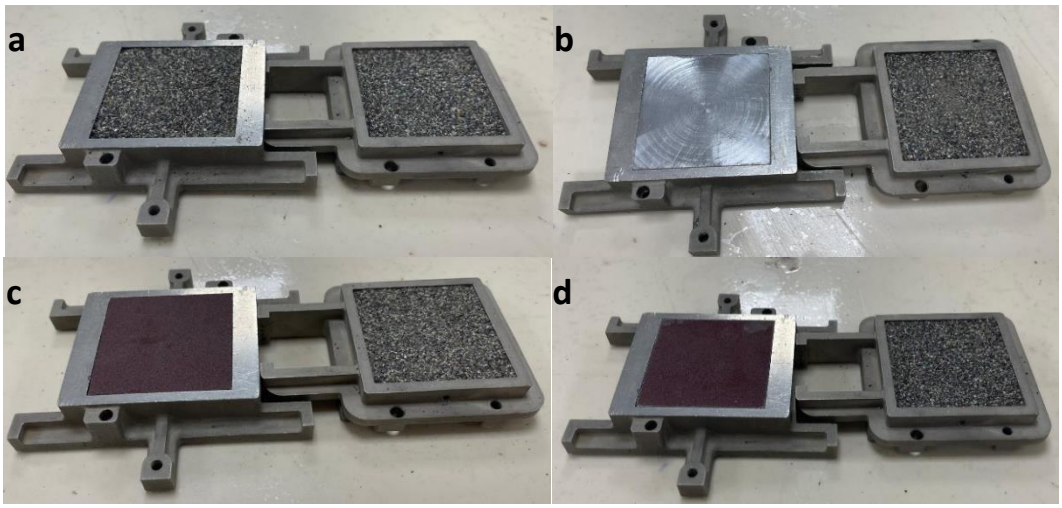

Figure 4. Sand-sand and pile – sand interface direct shear test samples: a) Sand – sand interface; b) Smooth pile – sand interface c) Medium pile-sand interface; d) Rough pile-sand interface

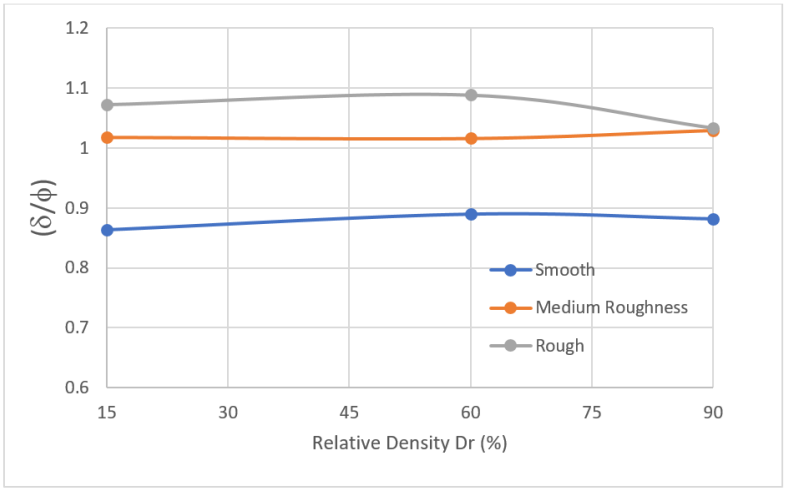

Figure 5. Effects of relative density and interface roughness on ratio (δ/ϕ)

Load-Displacement Curves and Summary of Results

The pullout test was conducted 27 times, and uplift load-vertical displacement curves under different conditions were achieved. Franke (1985) and Ismael (1989) defined the ultimate pullout capacity as the maximum load achieved over the test before pile draw out. Figures 6, 7 and 8 show the load-displacement curves for various geometry parameters (L/D) of 10, 20 and 30, respectively. The model pile resistance mobilized rapidly with a few mm (small displacement) due to the high effective lateral stress on the pile surface, which rapidly mobilizes friction along the soil–pile interface. As the L/D ratio increases, the pile length increases, providing a larger shaft area to develop resistance. Consequently, the displacement required to reach the ultimate pullout load also increases slightly. The results demonstrate that the axial displacement to gain the ultimate pullout load ranged between (0.39-1.69), (0.67-4.73) and (0.64-6.66) mm for (L/D) ratios of 10, 20 and 30, respectively. For all (L/D) ratios, the minimum displacement observed for smooth model piles embedded in loose sand (LS10, LS20 and LS30) as the soft soil easily shears, and the smooth shaft has lower interface friction, so friction is mobilized at a very small movement. The maximum displacement was achieved in rough model piles embedded in medium soil for (L/D) ratios of 10 and 20 (MR10 and MR20), because higher interface friction requires more displacement to fully mobilize shaft resistance, while the smooth pile model embedded in dense sand (DS30) exhibits larger displacement for (L/D) = 30. The performance of model pile with (L/D) ratio of 30 embedded in dense sand depends upon the high friction interface that mobilizes quickly in medium and rough shaft skin at shorter displacements that would be sufficient to reach ultimate shaft resistance along the pile. On the other hand, smooth surface has lower friction per unit area; full mobilization along the pile requires more axial displacement.

The behavior of tension piles can be categorized as either brittle or ductile, with the normalized displacement (s/D) frequently utilized to define these responses. Brittle failure usually manifests at very small displacements, where (s/D) values range from approximately 0.01 to 0.05. In this failure mode, piles undergo a swift reduction in load-carrying capacity with little forewarning prior to failure, a phenomenon often seen in dense sands (Alawneh et al., 2019; Lehane & White, 2005). Conversely, ductile failure progresses gradually over larger displacements, with (s/D) values typically falling between 0.1 and 0.3, and in certain very soft soils, reaching up to 0.5. This behavior permits gradual deformation before achieving ultimate load, offering warning signs and allowing for corrective actions. Ductile responses are frequently observed in soft clays or loose sands (White & Lehane, 2004; Chen et al., 2022). A summary of the normalized displacements (s/D) is demonstrated in Table 4. Generally, the normalized displacement that mobilized the failure over the conducted 27 tests ranged between (0.026-0.444). The results demonstrate that the combined effect of soil density, pile model roughness and slenderness ratio is highly affecting the failure behavior (brittle or ductile) of the tension pile.

A summary of the ultimate model pile capacities is assembled in groups (see Table 5). Regarding model pile skin roughness and geometry ratio (L/D), they are represented graphically in Figure 9 for an excessive discussion in terms of ultimate uplift development index (UUDI), considering geometry parameter (L/D) = 10 as a reference.

$$\mathrm{UUDI} = \frac{Q_{ult,(\frac{L}{D})}}{Q_{ult,(\frac{L}{D}=10)}}.$$

Generally, an increase in the geometry ratio (L/D) expresses a noticeable increase in the ultimate uplift capacity, with a minimum UUDI of 2.67 observed when a smooth model pile is embedded in loose sand (LS30), while the maximum UUDI of 14.90 is achieved for a medium rough model pile embedded in dense sand (DU30). Regarding increasing the relative density, moderate improvement was depicted as UUDI ranged between (0.33 – 6.0) for model piles MR10 and DS30, respectively. The increase in relative density signifies noticeable improvement in ultimate uplift capacity regarding the increase in interface friction angle (δ), especially for model pile DU30 and DR30, but model pile DU30 gains its ultimate state at upward displacement more than that of DR30 due to its high interface friction, as explained previously. Furthermore, the increase in relative density reveals a sharp increase in the ultimate uplift capacity for R30 and U30 groups due to high friction resistance and interface friction, while S30 gains a significant increase. Moderate increase is observed over groups S20, U20 and R20 and

a marginal improvement is achieved when geometry ratio (L/D) = 10 (S10, U10 and R10). Despite remarkable increase in ultimate uplift capacity due to a change in model pile skin roughness, the results indicate marginal improvement compared to that of smooth pile skin. The minimum UUDI of 0.11 was achieved when the model pile with medium roughness was driven in dense soil (DU10), while the maximum index of 2.81 was recorded when the rough pile model was embedded in loose sand (SR30). Successful selection of tension pile has to be decided depending on the ultimate limit of both vertical displacement and pullout load, effectively controlled by a combination of geometry ratio, soil density and pile roughness.

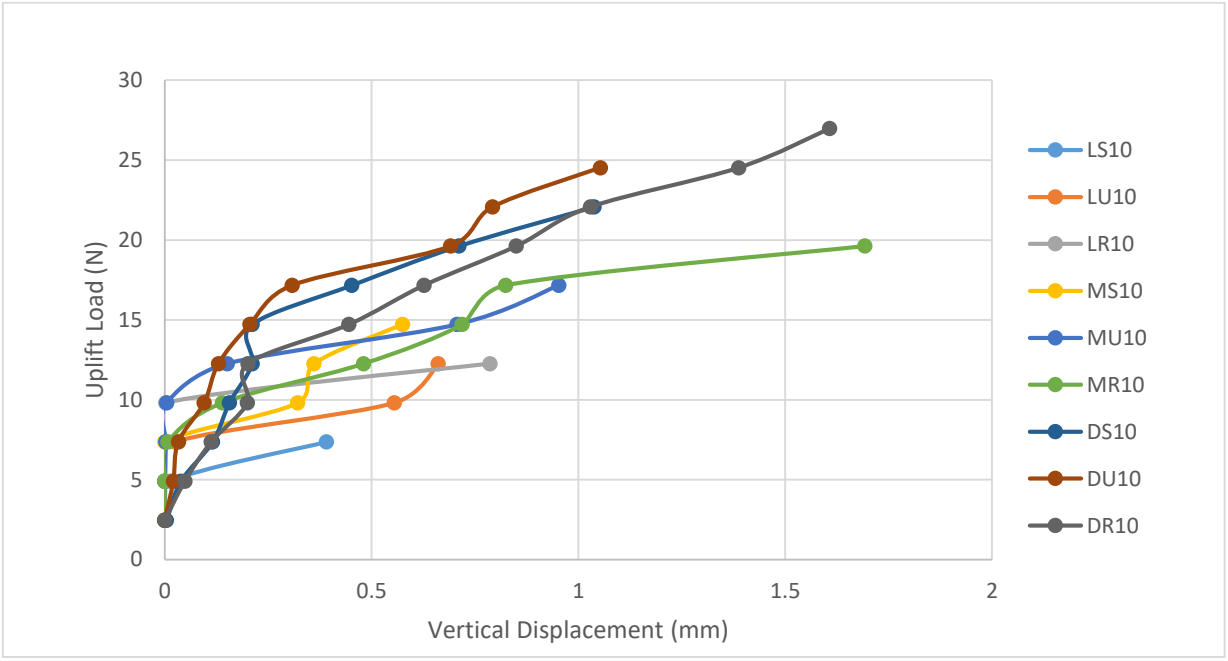

Figure 6. Load – displacement curve for geometry parameter (L/D) = 10

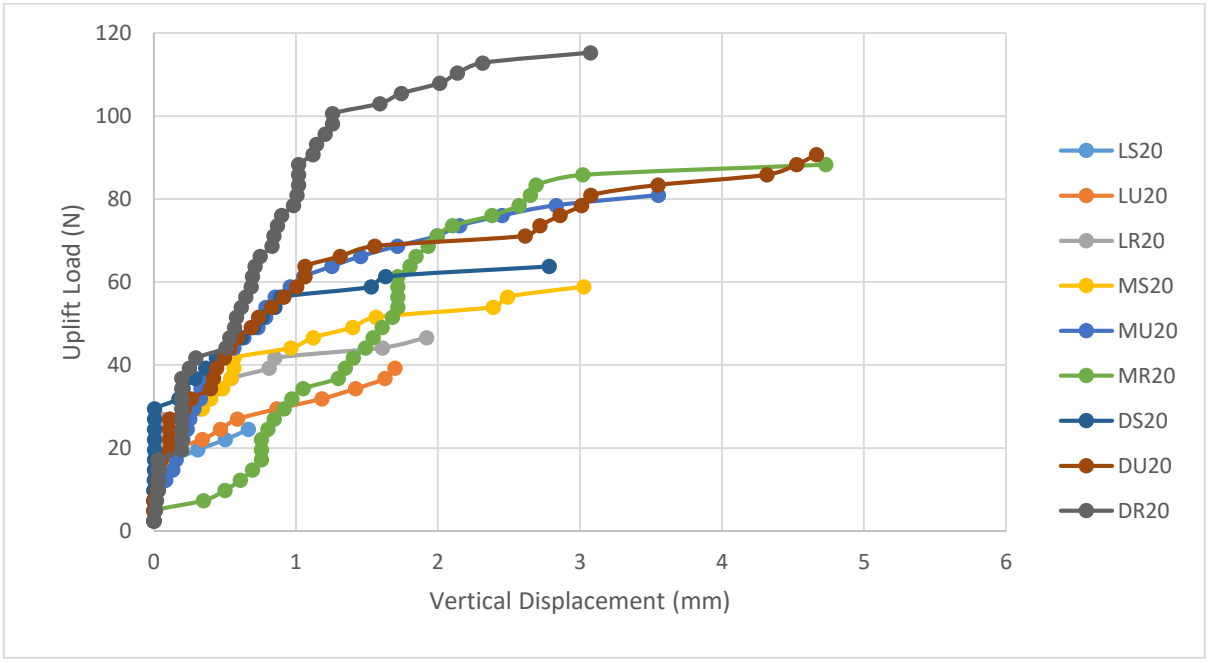

Figure 7. Load – displacement curve for geometry parameter (L/D) = 20

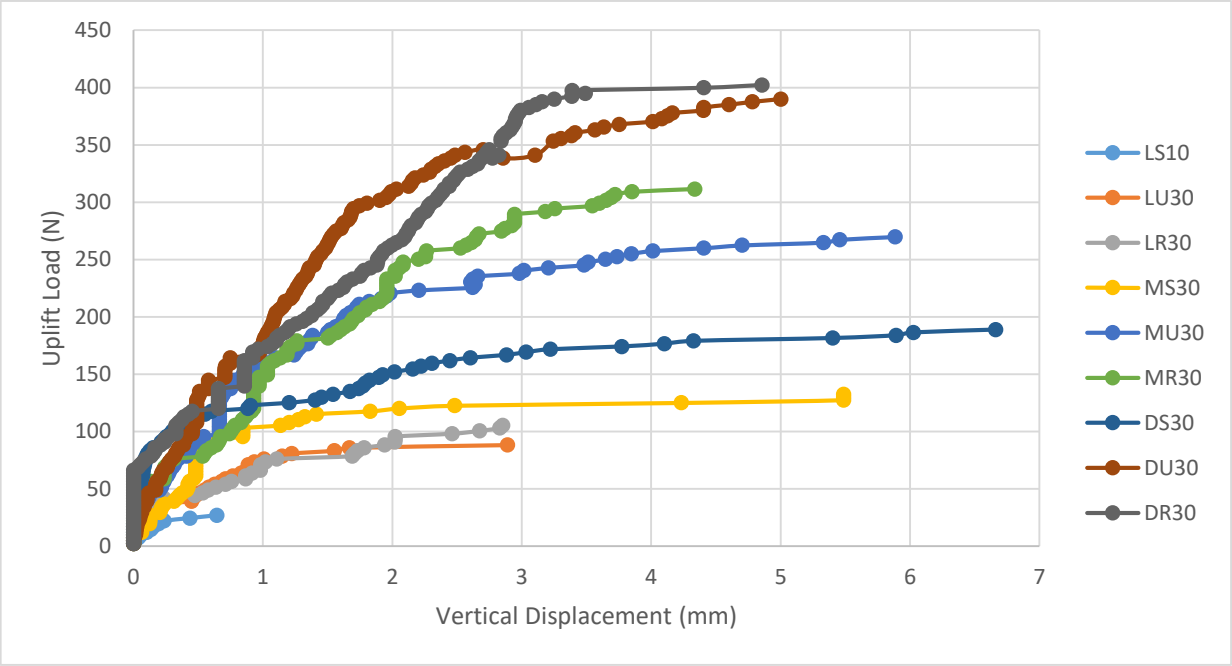

Figure 8. Load – displacement curve for geometry parameter (L/D) = 30

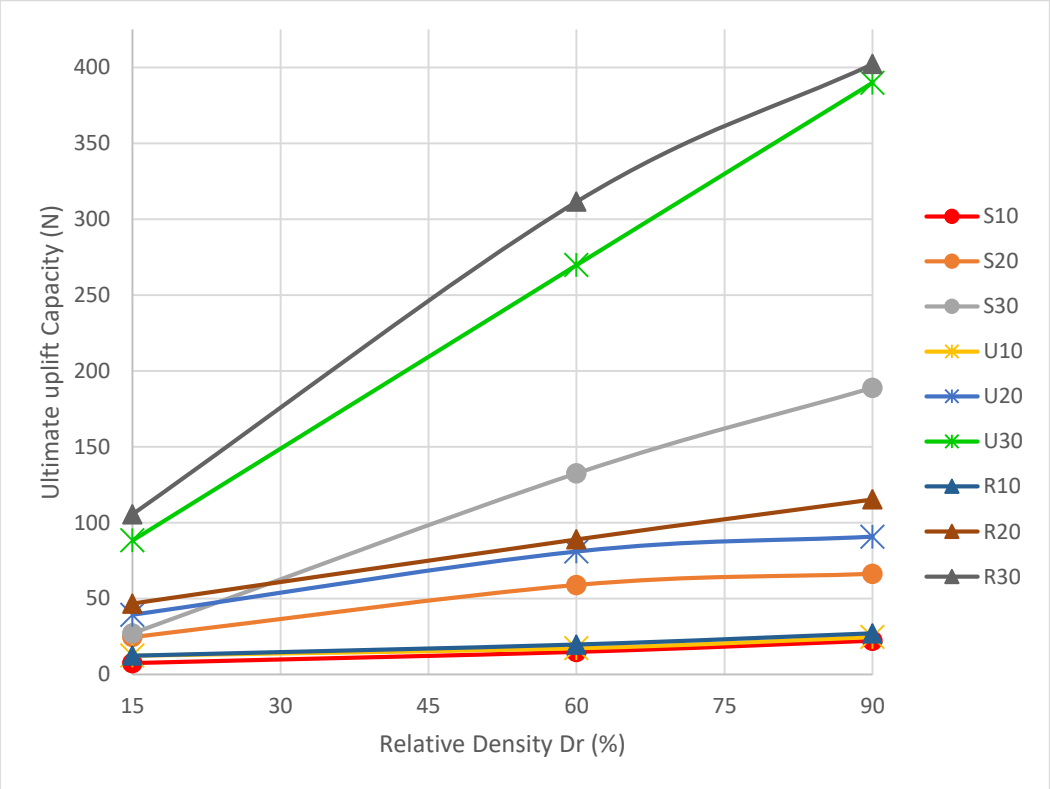

Figure 9. Ultimate uplift capacity summary

Table 4. Normalized displacement summary

Pile Skin Roughness	L/D	Identification Code	Soil State		
			15	60	90
Smooth (S)	10	S10	0.026	0.038	0.069
	20	S20	0.044	0.202	0.186
	30	S30	0.043	0.366	0.444
Medium (U)	10	D10	0.044	0.064	0.070
	20	D20	0.113	0.237	0.311
	30	D30	0.193	0.392	0.333
Rough (R)	10	R10	0.052	0.113	0.107
	20	R20	0.128	0.315	0.205
	30	R30	0.190	0.289	0.324

Table 5. Ultimate uplift capacity summary

Pile Skin Roughness	L/D	Identification Code	Soil State		
			Loose (L)	Medium (M)	Dense (D)
Smooth (S)	10	S10	7.36	14.72	22.07
	20	S20	24.53	58.86	66.22
	30	S30	26.98	132.44	188.84
Medium (U)	10	D10	12.26	17.17	24.53
	20	D20	39.24	80.93	90.74
	30	D30	88.29	269.78	389.95
Rough (R)	10	R10	12.26	19.62	26.98
	20	R20	46.60	88.9	115.27
	30	R30	105.46	311.47	402.21

** Ultimate uplift capacity is presented in (N).*

CONCLUSIONS

Based on the results and discussion of 27 pullout tests, the following conclusions can be drawn:

1. The ratio of interface friction to internal friction (δ/ϕ) increases in accordance with increasing pile skin roughness, with no significant effect to the change in relative density for a proper roughness state, except that of dense soil – rough skin, which reduced due to high friction resistance.
2. Generally, the pullout displacement required to reach ultimate load increased with increasing pile slenderness ratio (L/D) and interface friction. The uplift displacement that mobilized failure across all tests ranged between (2.6%-44.5%) of pile diameter, which provides a practical measure for allowable displacements in design.
3. Increasing the L/D ratio enhanced ultimate uplift capacity, with a maximum UUDI of 14.90 achieved as a combined effect of a medium rough model pile embedded in dense sand at a slenderness ratio of 30.
4. Increasing relative density and slenderness ratio improved uplift resistance, particularly for rough and medium-rough piles, with sharp improvements at L/D = 30, moderate improvements at L/D = 20, and only marginal changes at L/D = 10.
5. Pile surface roughness significantly affected uplift performance, with rough and medium-rough piles outperforming smooth piles; however, in some conditions, the improvement was marginal. Artificial roughening of pile shafts (e.g. coating, surface treatment) may be an economical solution to

enhance uplift resistance in sandy soils.

6. The slenderness ratio has a significant effect on the developed uplift tension capacity compared to soil density and pile skin roughness, which have moderate and marginal effects, respectively.
7. Allowable displacement criteria should be incorporated in design alongside ultimate capacity, since high capacity may be achieved at displacements that are not tolerable for structures.
8. The combination of soil density, pile roughness, and slenderness ratio significantly influences the failure mode (brittle or ductile).
9. Additional studies considering the combined effect of other parameters, like rising and lowering of the water table, cyclic or seismic loading, are suggested to better understand long-term uplift behavior, as well as numerical simulations to generalize experimental observations.

REFERENCES

Alawneh, A.S. (1999). Tension piles in sand: A method including degradation of shaft friction during driving (Paper No. 99-0092). *Transportation Research Record, 1663*, 41-49. National Research Council.

Alawneh, A.S., Malkawi, A.I.H., & Al-Deeky, H. (1999). Tension tests on smooth and rough model piles in dry sand. *Canadian Geotechnical Journal, 36*(4), 746-753. https://doi.org/10.1139/t98-104

Alawneh, A., Nusier, O., & Atiyeh, M. (2019). A new approach for estimating capacity of driven piles in sand under tensile loading. *Jordan Journal of Civil Engineering, 13*(3), 412-430.

Al-Mhidib, A., & Edil, B. (1999). Effect of pile installation method on uplift capacity of piles in sand. In *Proceedings of the Fourth Saudi Engineering Conference* (pp. 73-79). Jeddah, Saudi Arabia.

ASTM International. (2007). *ASTM D422-63: Standard test method for particle-size analysis of soils*. West Conshohocken, PA: Author.

ASTM International. (2014). *ASTM D854-14: Standard test methods for specific gravity of soil solids by water pycnometer*. West Conshohocken, PA: Author.

ASTM International. (2010). *ASTM D4253-4254: Standard test method for maximum and minimum index density and unit weight of soils using a vibratory table*. West Conshohocken, PA: Author.

ASTM International. (2011). *ASTM D3080/D3080M-11: Standard test method for direct shear test of soils under consolidated drained conditions*. West Conshohocken, PA: Author.

ASTM International. (2020). *ASTM D2487-17: Standard practice for classification of soils for engineering purposes (Unified Soil Classification System)*. https://doi.org/10.1520/D2487-17

Azzam, W. R., & Al Mesmary, M. (2010). The behavior of single tension pile subjected to surcharge loading. *NED University Journal of Research, 7*(1), 1-12.

Azzam, W., & Elwakil, A. (2016). Model study on the performance of single-finned pile in sand under tension loads. *International Journal of Geomechanics, 17*(3), 04016072. https://doi.org/10.1061/(ASCE)GM.1943-5622.0000761

Azzam, W.R., & Basha, A. (2017). Utilization of soil nailing technique to increase shear strength of cohesive soil and reduce settlement. *Journal of Rock Mechanics and Geotechnical Engineering, 9*(6), 1104-1111. https://doi.org/10.1016/j.jrmge.2017.05.009

Basha, A., & Azzam, W. (2018). Uplift capacity of single pile embedded in partially submerged sand. *KSCE Journal of Civil Engineering, 22*, 1-9. https://doi.org/10.1007/s12205-017-1715-2

Chattopadhyay, B. C., & Pise, P. J. (1986). Uplift capacity of piles in sand. *Journal of Geotechnical Engineering, 112*(9), 888-904.

Chen, C., Yang, Q., Leng, W., Dong, J., Xu, F., Wei, L., & Ruan, B. (2022). Experimental investigation of the mechanical properties of the sand-concrete pile interface considering roughness and relative density. *Materials, 15*(13), 4480. https://doi.org/10.3390/ma15134480

Das, B. M., & Sivakugan, N. (2019). *Principles of foundation engineering* (9th edn.). Cengage Learning.

Das, B.M., & Rozendal, D. B. (1983). Ultimate uplift capacity of piles in sand. *Transportation Research Record, 945*, 40-44. Washington, DC: Transportation Research Board, National Research Council.

Das, B. M. (1983). A procedure for estimation of uplift capacity of rough piles. *Soils and Foundations, 23*(3), 122-126.

Devashish, B.K., Kumavat, A.K., & Dalwadi, B.R. (2020). A review of uplift load carrying capacity and failure mechanism of cylindrical and belled pile. *International Research Journal of Engineering and Technology, 7*(4).

Franke, E., & Muth, G. (1985). Scale effect in 1g model tests on horizontally loaded piles. In *Proceedings of the 11th International Conference on Soil Mechanics and Foundations* (Vol. 2, pp. 1011-1014). Balkema.

Gaaver, K. (2013). Uplift capacity of single piles and pile groups embedded in cohesionless soil. *Alexandria Engineering Journal, 52*(3), 365-372. https://doi.org/10.1016/j.aej.2013.01.003

Ismael, N.F. (1989). Field test on bored piles subjected to axial and oblique pull. *Journal of Geotechnical Engineering, 115*(11), 1588-1598. https://doi.org/10.1061/ (ASCE)0733-9410(1989)115:11(1588)

Kranthikumar, A., Sawant, V.A., & Shukla, S. K. (2016). Numerical modeling of granular anchor pile system in loose sandy soil subjected to uplift loading. *International Journal of Geosynthetics and Ground Engineering, 2*(2), 1-15. https://doi.org/10.1007/s40891-016-0056-4

Kulhawy, F.H., Kozera, D.W., & Withiam, J.L. (1979). Uplift testing of model drilled shafts in sand. *Journal of the Geotechnical Engineering Division, 105*, 31-47.

Lehane, B.M., & White, D.J. (2005). Lateral stress changes and shaft friction for model displacement piles in sand. *Canadian Geotechnical Journal, 42*(4), 1039-1052. https://doi.org/10.1139/T05023

Lepage, S., & Boulon, M. (2010). Soil-structure interface behaviour: Laboratory tests and numerical modeling. *Computers and Geotechnics, 37*(5), 757-768. https://doi.org/10.1016/j.compgeo.2009.12.008

Meyerhof, G.G., & Adams, J.I. (1968). The ultimate uplift capacity of foundations. *Canadian Geotechnical Journal, 5*(4), 225-244.

Nazir, A.K. (2008). Effect of installation method on uplift capacity of piles in sand. *Alexandria Engineering Journal, 23*(3), 156-167.

Parthipan, N., & M.K. (2017). Experimental study on uplift load carrying capacity of steel pile in sand. *International Journal of Science and Research, 6*.

Robinsky, E.I., & Morrison, C.F. (1964). Sand displacement and compaction around model friction piles. *Canadian Geotechnical Journal, 1*(2), 81-93. https://doi.org/10.1139/t64-002

Shanker, K., Basudhar, P.K., & Patra, N.R. (2007). Uplift capacity of single piles: Predictions and performance. *Geotechnical and Geological Engineering, 25*(2), 151-161. https://doi.org/10.1007/s10706-006-9000-z

Shark, A., & Patra, R. (2008). Effect of arching on uplift capacity of single piles. *International Journal of Geomechanics, 8*(6), 347-354. https://doi.org/10.1007/s10706-008-9236-x

Srivastava, K., Singh, V.K., Yadav, A., Shelke, A., & Patra, N.R. (2008). Prediction of load-displacement response of single pile under uplift load: A comparative study. In *Proceedings of the 12th International Conference of the International Association for Computer Methods and Advances in Geomechanics (IACMAG)* (pp. 3408-3414). Goa, India.

Tehrani, F. S., Han, F., Salgado, R., Prezzi, M., Tovar, R. D., & Castro, A. G. (2016). Effect of surface roughness on the shaft resistance of non-displacement piles embedded in sand. *Géotechnique, 66*, 386-400.

Van Baars, S., & Niekerk, W.J. (2019). Numerical modelling of tension piles. In *Proceedings* (pp. 237-246). https://doi.org/10.1201/9781315138206-23

White, D. J., & Lehane, B. M. (2004). Friction fatigue on displacement piles in sand. *Géotechnique, 54*(10), 645-658. https://doi.org/10.1680/geot.2004.54.10.645

You, S., Lee, K., & Hong, G. (2024). Influence of fines content and pile surface characteristics on the pullout resistance performance of piles. *Materials, 17*, 124. https://doi.org/10.3390/ma17010124